

Operando Synchrotron Imaging of Electrolyte Distribution in Silver-based Gas Diffusion Electrodes during Oxygen Reduction Reaction in Highly Alkaline Media

Melanie Cornelia Paulisch^{1*}, Marcus Gebhard², David Franzen³, André Hilger¹, Markus Osenberg⁴, Shashidhara Marathe⁵, Christoph Rau⁵, Barbara Ellendorff³, Thomas Turek³, Christina Roth² and Ingo Manke¹

¹ Institute of Applied Materials, Helmholtz-Zentrum Berlin für Materialien und Energie GmbH, Hahn-Meitner-Platz 1, 14109 Berlin, Germany

² Electrochemical Process Engineering, University Bayreuth, Universitätsstraße 30, 95447 Bayreuth, Germany

³ Institute of Chemical and Electrochemical Process Engineering, Clausthal University of Technology, Leibnizstrasse 17, 38678 Clausthal-Zellerfeld, Germany

⁴ Department of Materials Science and Technology, Technical University Berlin, Hardenbergstr. 36, 10623 Berlin, Germany

⁵ Diamond Light Source Ltd Harwell Science & Innovation Campus, Didcot Oxfordshire OX11 0DE, United Kingdom

* Correspondence: melanie.paulisch@helmholtz-berlin.de

Abstract

Understanding how gas diffusion electrodes are working is crucial to improve their performance and cost efficiency. One key issue is the electrolyte distribution during operation. Here, operando synchrotron imaging of the electrolyte distribution in silver-based gas diffusion electrodes is presented. For this purpose, a half-cell compartment was designed for operando synchrotron imaging of chronoamperometric measurements. For the first time the electrolyte distribution could be analyzed in real time (1 s time resolution) even in individual pores as small as a few μm . The detailed analyses of dynamic filling processes are an important step for understanding and improvement of electrodes.

Keywords: in situ/operando techniques; synchrotron imaging; gas diffusion electrode; oxygen-depolarized cathode; oxygen reduction reaction; electrolyte distribution

Chlorine is one of the most important base chemicals in the chemical industry. Its production is mainly based on the very energy-intensive chlor-alkali electrolysis. The energy demand can be reduced up to 30 %¹ by introducing the so-called oxygen depolarized cathode technology to the state of the art membrane process. By the usage of metallic gas diffusion electrodes (GDEs)² the oxygen reduction reaction (ORR) instead of the hydrogen evolution is catalyzed. This is an important step regarding the environmental sustainability and will help to comply with future emission limits^{1, 3-5}. Therefore, the development of metallic GDEs, which can be used in highly alkaline electrolytes and deliver the required high performance, is an essential key topic. and led to the development of porous silver-based GDEs⁶⁻⁸. Detailed microstructural analyses of such GDEs revealed silver grains, which are surrounded by a complex pore network and polytetrafluoroethylene (PTFE), located at the **silver-air interfaces**⁹. It is expected that the hydrophilic silver grains support the spreading of the electrolyte (30 wt.% NaOH) inside the GDE, while the hydrophobic PTFE keeps the pore paths free for the gas phase⁷. The Influence of the microstructure on the electrochemical behavior were already analyzed in detail⁹⁻¹². To analyze the electrolyte distribution within the GDE, Gebhard et al.¹³ designed a half-cell compartment, which is optimized for electrochemical measurements and X-ray radiography. Investigations by Paulisch et al.¹¹ showed that the electrolyte amount within the GDE is dependent on the overpotential. High overpotentials cause fast electrolyte penetration and spreading within the GDE due to electro wetting. As these analyses led to integral results only, a more detailed visualization of the pore network system during operando measurements is needed to understand the electrolyte distribution and motion within the electrode. Therefore, in this study operando

electrochemical investigations have been carried out at the synchrotron facility Diamond Light Source (DLS), Oxfordshire, United Kingdom.

The half-cell setup (Fig. 1a) consists of an electrolyte and a gas part. Between both parts the GDE is mounted. In this way one side of the electrode is in contact with electrolyte and the other with gas. The geometrical surface area and the field of view are 3.14 cm². The electrochemical measurements are not corrected regarding internal resistance. A detailed description of the cell design is given by Gebhard et al.¹³⁻¹⁴ and shown in Fig. 1a. For the electrochemical procedure 250 ml of 30.wt % NaOH electrolyte was circulated several times in a closed circuit with a flow rate of 33 mL min⁻¹ at room temperature, while the O₂ gas flow was maintained at 20 mL min⁻¹. The electrochemical potentials were measured against a reversible hydrogen electrode (RHE) in a three-electrode setup. The working electrode is the GDE which is to be analyzed. Here oxygen and water react together with electrons to form hydroxide ions (reduction):



The chronoamperometry measurements were carried out in steps at 0.2 V, 0.9 V, 0.5 V and 0.2 V vs. RHE. Each step was measured for 30 min. The production of the GDEs is explained in detail in the literature^{9, 15} (see also supplementary information) . For this investigation a 300 μm thick GDE with 97 wt.% Ag and 3 wt.% PTFE was used, as this chemical composition offers stable performances and has already been thoroughly investigated^{7, 9, 11, 15}. Fig. 1b-c show the microstructure of the GDE prepared by focused ion beam (FIB) and detected by scanning electron microscopy (SEM).

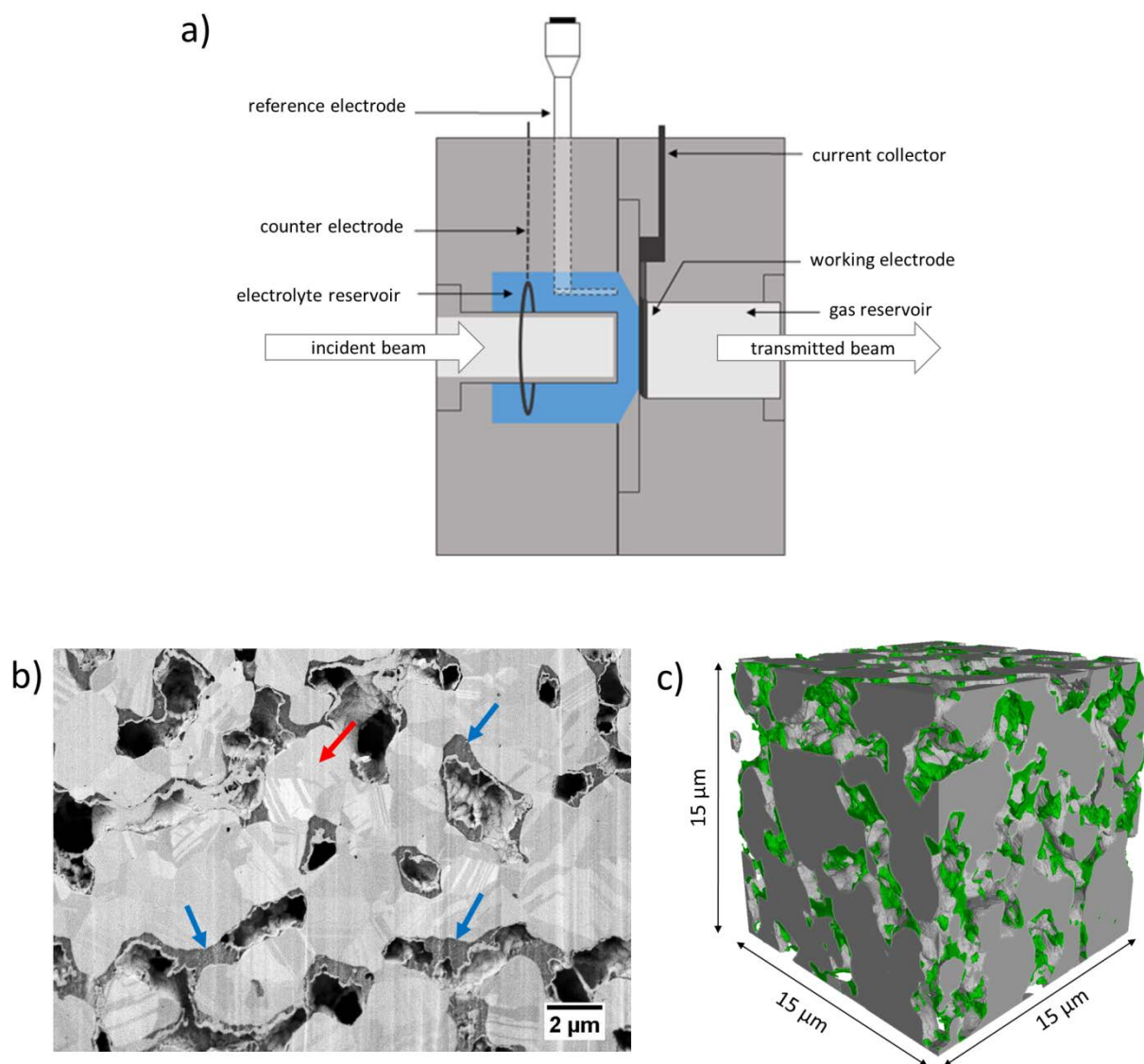


Fig. 1: a) Operando cell for chronoamperometry measurements¹¹ (reproduced with permission from reference 11. Copyright 2019 Materials, MDPI), b) FIB/SEM, microstructure of the GDE, Ag grains (red arrow) form a scaffold with a complex pore system and PTFE (blue arrows) at the silver-air interfaces, c) 3D FIB tomography, microstructure of the GDE, Ag grains (grey) with PTFE areas (green) within the pore system.

The synchrotron operando measurements were performed at the beamline I13-2 at DLS¹⁶⁻¹⁷. While operando synchrotron imaging measurements on metal-free electrodes were already demonstrated by Normile et al.¹⁸, this kind of measurement is extremely difficult for massive metal electrodes such as the silver GDEs shown here, due to the high attenuation coefficient of silver for X-rays. In order to realize these measurements, we used X-ray energies directly below the silver X-ray absorption edge to prevent excitation of the corresponding electronic

states. In this way a maximum transmission was achieved, while high sensitivity for the electrolyte was still ensured. For the measurements pink beam was applied. To shift the X-ray energy distribution to energies mainly below the k-edge of silver and also to avoid boiling of the electrolyte, foils of Ag (0.035 mm), Pd (0.042 mm), Al (2.12 mm) and Fe (0.04 mm) were used as filters. Together with the high intensity of the pink beam acceptable signal-to-noise ratios were achieved for measurements at 1 s time resolution and high spatial resolution (0.8 μm x 0.8 μm pixel size) at the same time. The gap of the U22 insertion device was set to 5 mm. The undulator harmonics were filtered and a horizontal deflecting rhodium coated mirror stripe under a deflection angle of 4.3 mrad. The images were taken with a pco.edge 5.5 camera in a field of view of 2.1 mm x 1.8 mm. The optical setup consisted of a UPlanFL N 4x objective (NA = 0.13) and a 500 μm LuAG:Ce doped scintillator. The software Fiji was used for image analysis (ImageJ 1.52p)¹⁹.

The correlation between electrochemical performance and electrolyte distribution within the GDE is shown in Fig. 2. In this analysis special attention is given to the question how the electrolyte distribution is affected by different electrochemical potentials, how fast the electrolyte can move inside the pore system of the GDE and in which regions differences of the fluctuation behavior are visible. Therefore, the term “temporal fluctuation change” is defined here as changes of the electrolyte distribution between two projections. It is the temporal derivative of the electrolyte distribution and a measure for the speed with which the electrolyte distribution changes²⁰. The temporal fluctuation change map highlights areas with strong temporal fluctuations of the electrolyte amount. The temporal fluctuation change $F_t(x, y)$ at a given pixel position (x, y) is defined as

$$F_t = \frac{1}{t \cdot N} \sum_{k=1}^N |d_{k+1}(x, y) - d_k(x, y)|,$$

where N is the total number of images for a chosen time frame, d the local transmission length through the electrolyte at a given pixel position (x, y) and t the exposure time of each image. If the electrolyte distribution does not change, the grey value $F_t = 0$ (see Alrwashdeh et al.²⁰ for more details).

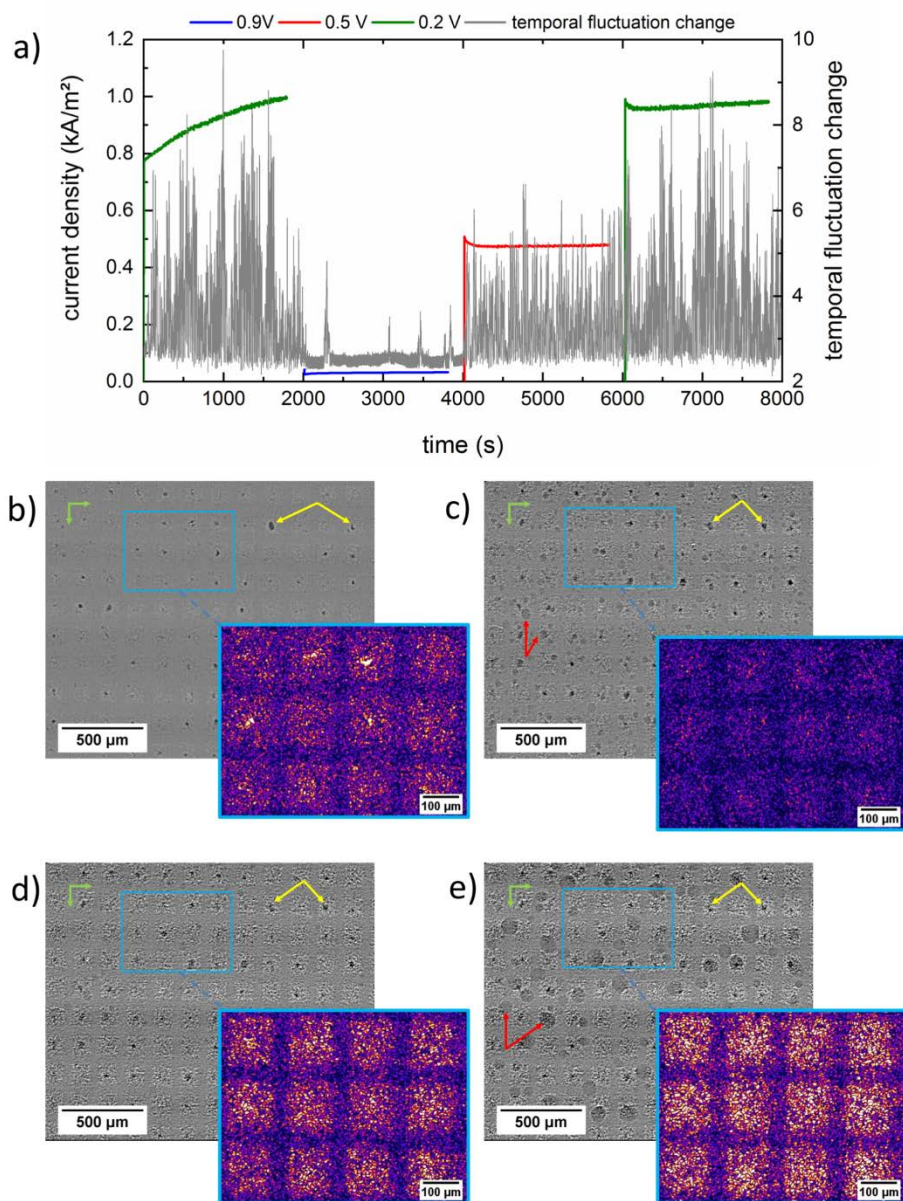


Fig. 2: Operando synchrotron imaging of the electrolyte in the GDE: a) correlation between chronoamperometry curves and electrolyte distribution, b) radiography and temporal fluctuation change map

(detail enlargement) of the GDE at 0.2 V, Ni mesh (green arrow), pores filled with electrolyte (yellow arrows), c) at 0.9 V, droplet formation (red arrows), d) at 0.5 V, e) at 0.2 V.

To visualize the distribution of the electrolyte within the GDE, the radiographic projections were normalized to projections of the filled cell without applied overpotential. Fig. 2a shows the current density at different applied potentials in correlation to the temporal fluctuation change of the GDE. It shows increasing current densities with increasing applied overpotential. Fig. 2b-e show radiographies of the GDE at different applied potentials and corresponding temporal fluctuation change maps in detail enlargements. When 0.2 V was applied the first time (Fig. 2b), the electrolyte enters into and spreads within the GDE. Large pores, located in the middle of the Ni mesh, fill up with electrolyte (yellow arrows). The temporal fluctuation change map shows high fluctuation changes in the region of large pores. At 0.9 V (Fig. 2c) the fluctuation changes within the GDE are quite low. However, the large pores stay filled, which is indicated by the low fluctuation changes in these areas. Moreover, Fig. 2c shows droplets formed on the gas side, which occurred at 0.2 V. At 0.5 V (Fig. 2d) the fluctuation changes of the GDE are increasing again. When 0.2 V is applied a second time (Fig. 2e) the fluctuation changes are further increased.

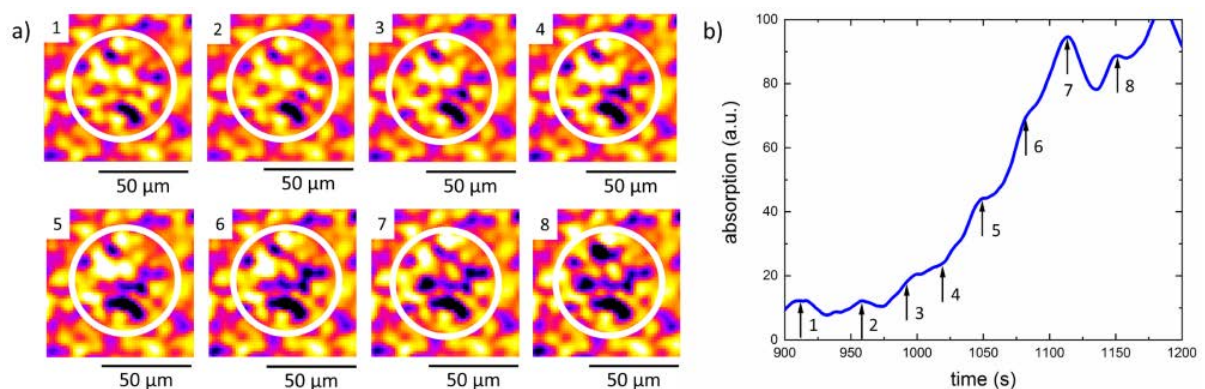


Fig. 3: a) Image series of a filling process at 0.2 V of a large pore system, white circles indicate the analyzed pore system; (white to orange low absorption, violet to black high absorption), b) absorption changes over the time

within the visualized pore system (ROI: $24\ \mu\text{m} \times 24\ \mu\text{m}$), arrows indicate the moment of exposure for the projections shown in a); the bump between position 7 and 8 was caused by beam variation.

Furthermore, it was possible to image the filling process of individual pores and the surrounding pore system at $0.2\ \text{V}$ over time. Fig. 3a shows the infiltration of the electrolyte into the pore system. For this image series the projections were referred to an image, which was taken shortly before the pore system got filled. Thus, only the changes of the electrolyte within the time period of filling are visualized. Areas, which are colored in white to orange, are those with low absorption, areas in violet to blue are those with high absorption. The higher the absorption, the more electrolyte is contained inside the GDE. Fig. 3b shows the changes of the absorption within the visualized pore system (region of interest (ROI): $24\ \mu\text{m} \times 24\ \mu\text{m}$). Due to the application of pink beam a quantification of the electrolyte volume is not reliably possible. After approximately 15 min electrolyte reaches the large pore system in the middle of the GDE and fills it up within 5 min. During this time complex filling processes were observed. The electrolyte spreads into discrete channels. Sometimes pores fill and go dry again while filling an adjacent pore and later get filled again. After the pores are filled, there are no changes in the overall distribution until the end of the measurement. There are paths that are preferably filled by the electrolyte. At the same time, other paths do not show changes in the absorption, which is a hint that these paths stay free of electrolyte and support the penetration with and spreading of oxygen.

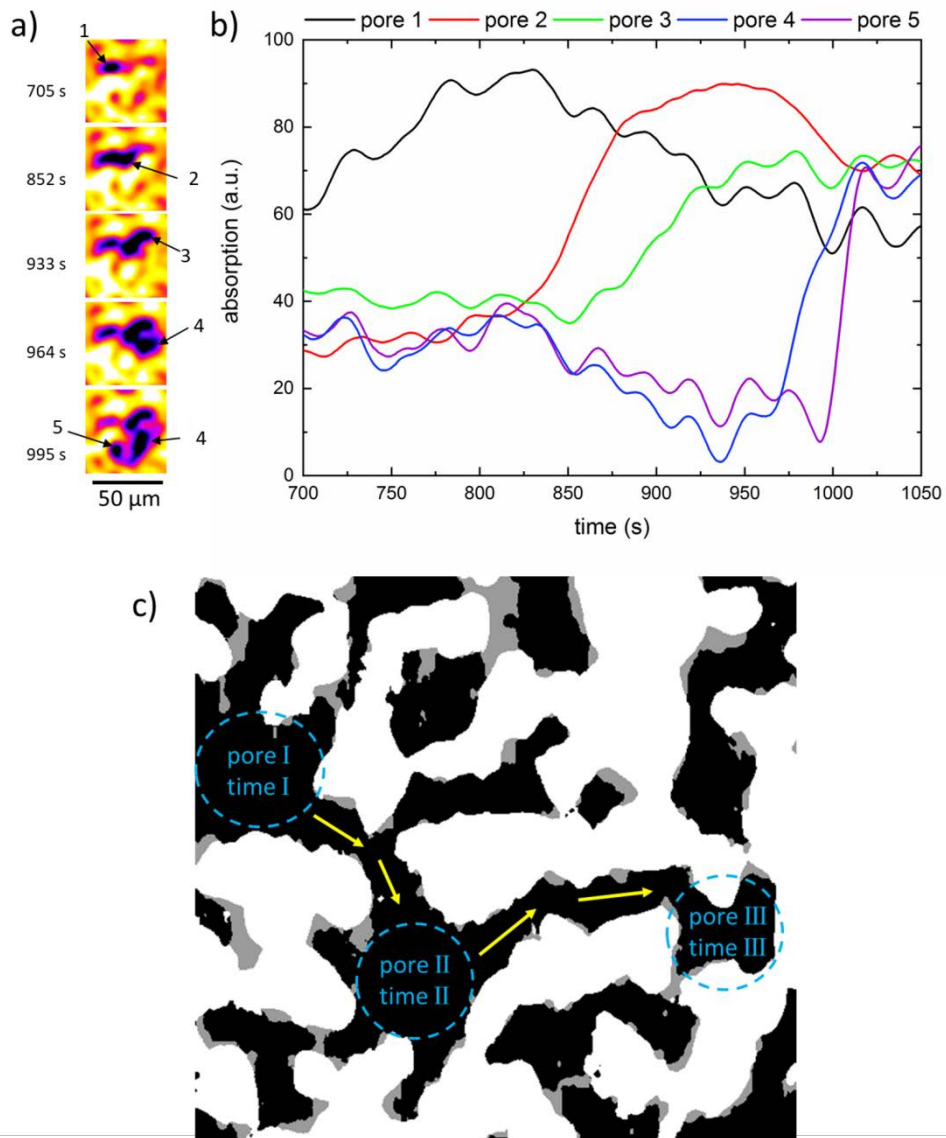


Fig. 4: Filling of a pore network with electrolyte at 0.2 V, a) electrolyte distribution between the 700st and the 1050th second (white to orange low absorption, violet to blue high absorption), b) absorption changes over the time indicating the filling process of selected pores (ROI: 4.7 μm x 4.7 μm), c) scheme of the GDE microstructure, Ag (white), PTFE (grey), pores (black) with an illustration of the filling process.

Fig. 4 shows the filling behavior of single pores at 0.2 V. As soon as the overpotential is applied, the electrolyte is able to enter the GDE. After 700 s and 830 s the pores in position 1 and 2 get filled with electrolyte. After the filling process the absorption for both positions is decreasing, indicating a declining electrolyte volume within the ROI (4.7 μm x 4.7 μm). This is a hint of electrolyte drainage from the large pore into the surrounding pore system. Another

possibility is that smaller pores in the transmission line are emptied again. The filling process in position 3 starts after 870 s. In this case a drainage effect is not visible. We found similar filling times for these three pores: 170 s for pore 1 and 2 and 125 s for pore 3, respectively. Pore 1 shows decreasing absorption when pores 2 and 3 get filled. The same behavior can be found also for pore 2. This is a hint towards a local rebalancing of the electrolyte distribution, i.e. that electrolyte flows off the area of pore 1 and 2 to fill other pores in the system. When the flooding of the pores 1 to 3 is completed, pore 4 and 5 get filled within 45 s and 30 s, respectively. After the filling and the drainage effect the intensity stays constant, which means the electrolyte volume is not changing significantly. Fig. 4c shows the scheme of the GDE's microstructure with an illustration of the filling process. The first pore gets filled at time I. The electrolyte flows along the yellow arrows through the pore path into pore II and afterwards into pore III at time III.

The question how media are distributed within electrodes is very important for understanding how they are working and how to improve their performances. For the first time it was possible to analyze the electrolyte distribution within silver-based GDEs in detail by synchrotron imaging. The analyses show mainly a continuous flow of the electrolyte similar to the observed water distribution in proton exchange membrane fuel cells²¹⁻²³. Regarding the larger pores the obvious assumption is that they act as reservoirs for the surrounding pore system. Similar effects were observed in polymer electrolyte membrane fuel cells. Alink et al.²⁴ and Haußmann et al.²⁵ show in this context that larger pores have a drainage effect on their surrounding area which supports the liquid water transport. Furthermore, the flow resistance of large pores is low and the electrolyte can infiltrate easily²⁶. Beyond these effects the observation of the stepwise filling of the pore system shown in Fig. 3 revealed that the pore channels which get filled stay filled. At the same time

the temporal fluctuation change maps in Fig. 2 show the same effect, however, the fluctuation changes at 0.5 V and 0.2 V are high, which indicates that the electrolyte quantity within the electrode is changing over time. Nevertheless, the electrolyte is always following its preferred paths. Paulisch et al.¹¹ observed an increased electrolyte amount within the GDE with increasing overpotential. Additionally, in this study was shown that the electrolyte distribution within the GDE is changing faster with increasing overpotentials (Fig. 2a). The reason for this behavior is the effect of electro wetting. The contact angle between electrode and electrolyte decreases with increasing overpotential, which leads to a stronger wetting and, therefore, to decreasing resistance against electrolyte penetration, spreading and percolation²⁷⁻²⁸. The detailed analysis of the electrolyte distribution is fundamental for developing models which are predicting the media distribution within the GDE during ORR in highly alkaline electrolyte, as shown by Franzen et al.²⁹. Until now, all existing models for oxygen reduction in silver-based GDEs for ORR assume a static electrolyte distribution. The measurements reveal that this might not be the case for all operating conditions^{12, 29}. Therefore, improved models which take the dynamic electrolyte movement into account are needed.

In conclusion, it was possible for the first time to measure the electrolyte distribution inside individual pores of catalytically active silver GDEs during operation inside a half-cell compartment with operando synchrotron X-ray imaging. The measurements of the integral fluctuation changes of the electrolyte and the detailed analyses of dynamic filling processes of individual pores were possible despite the high attenuation of the GDEs. Clear correlations between the electrolyte distribution and the applied overpotentials have been revealed. These investigations are an important step for an improved understanding of metallic GDEs.

Acknowledgements

The study was funded by Deutsche Forschungsgemeinschaft in the framework of the research unit “Multiscale analysis of complex three-phase systems: Oxygen reduction at gas-diffusion electrodes in aqueous electrolyte” (FOR 2397; MA 5039/3-1, MA 5039/3-2, RO 2454/16-1, RO 2454/16-2 and TU 89/13-1, TU 89/13-2). The authors want to thank the institution Diamond Light source. The experiment was carried out under the experiment MG21813-1.

References

1. Jörissen, J.; Turek, T.; Weber, R., Chlorherstellung mit Sauerstoffverzehrkatoden. *Chemie unserer Zeit* **2011**, *45*, 172-183.
2. Moussallem, I.; Jörissen, J.; Kunz, U.; Pinnow, S.; Turek, T., Chlor-alkali electrolysis with oxygen depolarized cathodes: history, present status and future prospects. *Journal of Applied Electrochemistry* **2008**, *38*, 1177-1194.
3. Kintrup, J.; Millaruelo, M.; Trieu, V.; Bulan, A.; Mojica, E. S., Gas Diffusion Electrodes for Efficient Manufacturing of Chlorine and Other Chemicals. *The Electrochemical Society Interface* **2017**, *26* (2), 73-76.
4. Garcia-Herrero, I.; Margallo, M.; Raquel, O.; Aldaco, R.; Irabien, A., Environmental challenges of the chlor-alkali production: Seeking answers from a life cycle approach. *Science of the Total Environment* **2017**, *580*, 147-157.
5. Jung, J.; Postels, S.; Bardow, A., Cleaner chlorine production using oxygen depolarized cathodes? A life cycle assessment. *Journal of Cleaner Production* **2014**, *80*, 46-56.
6. Chatenet, M.; Genies-Bultel, L.; Arousseau, M.; Durand, R.; Andolfatto, F., Oxygen reduction on silver catalysts in solutions containing various concentrations of sodium hydroxide – comparison with platinum. *Journal of Applied Electrochemistry* **2002**, *32*, 1131-1140.
7. Moussallem, I.; Pinnow, S.; Wagner, N.; Turek, T., Development of high-performance silver-based GDE for chlor alkali electrolysis with oxygen depolarized cathodes. *Chemical Engineering and Processing: Process Intensification* **2012**, *2012*, 125-131.
8. Furuya, N.; Aikawa, H., Comparative study of oxygen cathodes loaded with Ag and Pt catalysts in chlor-alkali membrane cells. *Electrochimica Acta* **2000**, *45*, 4251-4256.
9. Franzen, D.; Ellendorff, B.; Paulisch, M. C.; Hilger, A.; Osenberg, M.; Manke, I.; Turek, T., Influence of binder content in silver-based gas diffusion electrodes on pore system and electrochemical performance. *Journal of Applied Electrochemistry* **2019**, *49*, 705-713.
10. Gebhard, M.; Tichter, T.; Franzen, D.; Paulisch, M. C.; Schutjajew, K.; Turek, T.; Manke, I.; Roth, C., Improvement of Oxygen-Depolarized Cathodes in Highly Alkaline Media by Electrospinning of Poly(vinylidene fluoride) Barrier Layers. *ChemElectroChem* **2020**, *7* (3), 830-837.
11. Paulisch, M. C.; Gebhard, M.; Franzen, D.; Hilger, A.; Osenberg, M.; Kardjilov, N.; Ellendorff, B.; Turek, T.; Roth, C.; Manke, I., Operando Laboratory X-Ray Imaging of Silver-Based Gas Diffusion Electrodes during Oxygen Reduction Reaction in Highly Alkaline Media. *Materials (Basel)* **2019**, *12* (17), 2686-1700.
12. Röhe, M.; Kubannek, F.; Krewer, U., Processes and Their Limitations in Oxygen Depolarized Cathodes: A Dynamic Model-Based Analysis. *ChemSusChem* **2019**, *12*, 2373-2384.

13. Gebhard, M.; Paulisch, M.; Hilger, A.; Franzen, D.; Ellendorff, B.; Turek, T.; Manke, I.; Roth, C., Design of an In-Operando Cell for X-Ray and Neutron Imaging of Oxygen-Depolarized Cathodes in Chlor-Alkali Electrolysis. *Materials (Basel)* **2019**, *12* (8), 1275-1288.
14. Gebhard, M. Untersuchung poröser Elektroden der Chlor-Alkali-Elektrolyse und Vanadium-Redox-Flow-Batterie mittels in-situ und operando Radiografie (Doctoral Thesis). Freie Universität Berlin, 2020.
15. Moussallem, I. Development of Gas Diffusion Electrodes for a New Energy Saving Chlor-Alkali Electrolysis Process (Doctoral Thesis). Clausthal University of Technology, 2011.
16. Rau, C., Coherent imaging at the Diamond beamline I13. *Physica Status Solidi A* **2011**, *208* (11), 2522-2525.
17. Rau, C., Imaging with Coherent Synchrotron Radiation: X-ray Imaging and Coherence Beamline (I13) at Diamond Light Source. *Synchrotron Radiation News* **2017**, *30* (5), 19-25.
18. Normile, S. J.; Sabarirajan, D. C.; Calzada, O.; Andrade, V. D.; Xiao, X.; Mandal, P.; Parkinson, D. Y.; Serov, A.; Atanassov, P.; Zenyuk, I. V., Direct observations of liquid water formation at nano- and micro-scale in platinum group metal-free electrodes by operando X-ray computed tomography. *Materials Today Energy* **2018**, *9*, 187-197.
19. Schindelin, J.; Arganda-Carreras, I.; Frise, E.; Kaynig, V.; Longair, M.; Pietzsch, T.; Preibisch, S.; Rueden, C.; Saalfeld, S.; Schmid, B.; al., e., Fiji: An open-source platform for biological-image analysis. *Nature Methods* **2012**, *9*, 676-682.
20. Alrwashdeh, S. S.; Markötter, H.; Haußmann, J.; Arlt, T.; Klages, M.; Scholta, J.; Banhart, J.; Manke, I., Investigation of water transport dynamics in polymer electrolyte membrane fuel cells based on high porous micro porous layers. *Energy* **2016**, *102*, 161-165.
21. Manke, I.; Hartnig, C.; Grünerbel, M.; Lehnert, W.; Kardjilov, N.; Haibel, A.; Hilger, A.; Banhart, J.; Riesemeier, H., Investigation of water evolution and transport in fuel cells with high resolution synchrotron x-ray radiography. *Applied Physics Letters* **2007**, *90* (174105), 1-3.
22. Manke, I.; Hartnig, C.; Kardjilov, N.; Messerschmidt, M.; Hilger, A.; Strobl, M.; Lehnert, W.; Banhart, J., Characterization of water exchange and two-phase flow in porous gas diffusion materials by hydrogen-deuterium contrast neutron radiography. *Applied Physics Letters* **2008**, *92* (24), 244101.
23. Fazeli, M.; Hinebaugh, J.; Bazylak, A., Investigating Inlet Condition Effects on PEMFC GDL Liquid Water Transport through Pore Network Modeling. *Journal of The Electrochemical Society* **2015**, *162* (7), F661-F668.
24. Alink, R.; Haußmann, J.; Markötter, H.; Schwager, M.; Manke, I.; Gerteisen, D., The influence of porous transport layer modifications on the water management in polymer electrolyte membrane fuel cells. *Journal of Power Sources* **2013**, *233*, 358-368.
25. Haußmann, J.; Markötter, H.; Alink, R.; Bauder, A.; Dittmann, K.; Manke, I.; Scholta, J., Synchrotron radiography and tomography of water transport in perforated gas diffusion media. *Journal of Power Sources* **2013**, *239* (0), 611-622.
26. Danner, T.; Eswara, S.; Schulz, V. P.; Latz, A., Characterization of gas diffusion electrodes for metal-air batteries. *Journal of Power Sources* **2016**, *324*, 646-656.
27. Jeanty, P.; Scherer, C.; Magori, E.; Wiesner-Fleischer, K.; Hinrichsen, O.; Fleischer, M., Upscaling and continuous operation of electrochemical CO₂ to CO conversion in aqueous solutions on silver gas diffusion electrodes. *Journal of CO₂ Utilization* **2018**, *24*, 454-462.
28. Burchardt, T., An evaluation of electrocatalytic activity and stability for air electrodes. *Journal of Power Sources* **2004**, *135*, 192-197.
29. Franzen, D.; Paulisch, M. C.; Ellendorff, B.; Manke, I.; Turek, T., Spatially resolved model of oxygen reduction reaction in silver-based porous gas-diffusion electrodes based on operando measurements. *Electrochimica Acta* **2021**, *375*, 137976.